

# Electrical conductivity of $\text{Na}_3\text{Zr}_2\text{Si}_2\text{PO}_{12}$ -doped sodium aluminosilicate glass

Y. SADAOKA, M. MATSUGUCHI, Y. SAKAI

*Department of Industrial Chemistry, Faculty of Engineering, Ehime University, Matsuyama 790, Japan*

S. NAKAYAMA

*Research and Development Centre, Fine Ceramics Division, Shinagawa Refractories Co. Ltd, Bizen 705, Japan*

To improve the electrical conductivity of sodium aluminosilicate glass and  $\text{Na}_3\text{Zr}_2\text{Si}_2\text{PO}_{12}$  crystal, crystal-glass composite systems were examined. For the ceramics with a lower content of the glass, the activation energy of ionic conduction was lowered and the conductivity enhanced by adding glass and the pre-exponential factor was lowered. Whilst the activation energy of ionic conduction of  $\text{Na}_2\text{O}-\text{Al}_2\text{O}_3-X\text{SiO}_2$  ( $X = 4, 6$ ) glasses could not be lowered to the limiting value of ca. 0.5 eV, the glass-based sample doped with  $\text{Na}_3\text{Zr}_2\text{Si}_2\text{PO}_{12}$  powder indicated that the high ionic conductivity and its activation energy was lowered to ca. 0.3 eV. The composite of  $\text{Na}_3\text{Zr}_2\text{Si}_2\text{PO}_{12}$  crystalline powder and sodium aluminosilicate glass is a useful material to the solid electrolyte.

## 1. Introduction

The discovery of  $\text{Na}_3\text{Zr}_2\text{Si}_2\text{PO}_{12}$  represented an important development in the field of solid electrolytes because it demonstrated that a three-dimensional framework structure was comparable to that of  $\beta$ -alumina. It has been shown that crystalline compounds with the composition  $\text{Na}_{1+x}\text{Zr}_2\text{Si}_x\text{P}_{3-x}\text{O}_{12}$  belong to the best fast sodium ion conductors. The composition with the highest ionic conductivity is the original solid solution system with  $1.8 \leq X \leq 2.4$  [1, 2]. Most of these compositions appear to be monoclinic at room temperature and rhombohedral, when their conductivities are comparable to  $\beta$ -alumina. Von Alpen *et al.* [3] have reported that the activation energy for ionic conduction changed in the temperature range of 410 to 450 K and this change was caused by the phase transition from the monoclinic into rhombohedral phase. The activation energy ( $\sim 0.21$  eV) for sodium ion conduction in the higher temperature region is comparable to that of  $\text{Na}-\beta$ -alumina (0.24 to 0.16 eV). Cava *et al.* [4] have reported that the change of activation energy for sodium ion conduction could not be removed by the partial replacement of heavy atoms ( $\text{Zr} \rightarrow \text{Th}, \text{Hf}$ ;  $\text{Si} \rightarrow \text{Ge}$ ;  $\text{P} \rightarrow \text{As}$ ) and similar results were reported by Takahashi *et al.* [5].

Recently there has been considerable interest in glass solid electrolytes [6]. Glasses present several advantages over crystalline materials for solid electrolyte and/or chemical sensor applications; ease of preparation into thin plates or thin coated elements, absence of grain boundaries and pores and isotropy. Hunter and Ingram [6] have examined sodium ion conduction in glass including silicates, borates, etc. and found that conductivity increases with optical

basicity, whilst the activation energy falls toward an apparent limiting value of ca. 0.52 eV. In addition, no further improvements to conductivity could be achieved, even by the use of special additives such as NaCl, NaF,  $\text{Al}_2\text{O}_3$  etc. For the cationic conduction mechanism in silica based glasses, Anderson and Stuart [7] have tried to estimate the activation energy of ionic conduction based on classical ionic crystal theory and elasticity theory. Whilst, activation energy was estimated on the basis of some assumptions, the estimated activation energy (ca. 0.7 eV) in sodium ion conduction was consistent with the reported values (0.50 to 0.75 eV) for sodium silicate and sodium aluminosilicate systems. More recently, sodium silicate glasses and glass-ceramics containing a modifier cation such as  $\text{Y}^{3+}$  and  $\text{Sn}^{4+}$  were examined as a superionic conductor [8-10] and activation energy could not be lowered by modification to 0.5 eV or below. This paper presents the results of a study of the composite of  $\text{Na}_3\text{Zr}_2\text{Si}_2\text{PO}_{12}$  crystalline powder and sodium aluminosilicate glass to prepare the ionic conductor with a lower activation energy which is not affected by the operating temperature.

## 2. Experimental details

$\text{Na}_3\text{Zr}_2\text{Si}_2\text{PO}_{12}$  crystalline powder was made from reagent-grade  $\text{Na}_2\text{CO}_3$ ,  $\text{NH}_4\text{H}_2\text{PO}_4$ ,  $\text{ZrO}_2$  and  $\text{SiO}_2$  using conventional ceramic techniques. The raw materials were ball-milled with ethanol, dried at  $100^\circ\text{C}$ , calcinated in air for 4 h at  $900^\circ\text{C}$ , then ground. Pellets were pressed at  $1000 \text{ kg cm}^{-2}$  and sintered in air for 15 h at  $1250^\circ\text{C}$ . The powder was prepared by milling the sintered ceramics;  $\text{Na}_2\text{O}-\text{Al}_2\text{O}_3-X\text{SiO}_2$  ( $X = 2, 4, 6, 8$ ) was made from reagent grade  $\text{Na}_2\text{CO}_3$ ,  $\text{Al}_2\text{O}_3$  and  $\text{SiO}_2$  by sintering between  $1000^\circ\text{C}$

and 1350°C depending on the composition. The powder was also obtained by milling. The composite in the prescribed weight ratio was compressed at 200 kg cm<sup>-2</sup> and sintered for 2 h at 1000°C.

The prepared pellets were shaped to 10 mm × 10 mm with 0.5 mm thickness. Next, gold electrodes, 4 mm × 4 mm, were applied to opposite faces of the sheet by vacuum evaporation. The electrical properties were measured using an LCZ meter (100 Hz to 100 kHz) in N<sub>2</sub> flow (50 ml min<sup>-1</sup>) from room temperature to 330°C.

The crystalline phases were identified at room temperature by the standard X-ray diffraction (XRD) technique. The microstructure of the sample was examined using scanning electron microscopy.

### 3. Form of samples

The prepared sodium aluminosilicates were examined by the XRD technique. Na<sub>2</sub>O–Al<sub>2</sub>O<sub>3</sub>–2SiO<sub>2</sub> was identified as Carnegieite (low form) and no distinct glass phases were detected. For Na<sub>2</sub>O–Al<sub>2</sub>O<sub>3</sub>–6SiO<sub>2</sub> and Na<sub>2</sub>O–Al<sub>2</sub>O<sub>3</sub>–8SiO<sub>2</sub>, the broad band which indicates the existence of the glass phase was observed with the strong peaks ( $d = 4.262, 3.343 \text{ \AA}$ ) assigned to  $\alpha$ -quartz. For Na<sub>2</sub>O–Al<sub>2</sub>O<sub>3</sub>–4SiO<sub>2</sub>, the broad band and some weak diffraction patterns were observed. In addition, it was confirmed that Na<sub>3</sub>Zr<sub>2</sub>Si<sub>2</sub>PO<sub>12</sub> was identified in its monoclinic form with ZrO<sub>2</sub> as an impurity. The XRD patterns for the starting materials and composites are summarized in Table I. Hereafter, a specimen of Na<sub>3</sub>Zr<sub>2</sub>Si<sub>2</sub>PO<sub>4</sub> with  $X$  wt % of Na<sub>2</sub>O–Al<sub>2</sub>O<sub>3</sub>–4SiO<sub>2</sub> will be referred to as NASICON-XNA4S. Most XRD patterns observed in composites with Na<sub>2</sub>O–Al<sub>2</sub>O<sub>3</sub>–4SiO<sub>2</sub> were assigned to Na<sub>3</sub>Zr<sub>2</sub>Si<sub>2</sub>PO<sub>12</sub> and the  $d$ -values were scarcely influenced by the addition of Na<sub>2</sub>O–Al<sub>2</sub>O<sub>3</sub>–4SiO<sub>2</sub> glass. Fig. 1 shows some views of the microstructure of the sintered samples. While the form of the Na<sub>3</sub>Zr<sub>2</sub>Si<sub>2</sub>PO<sub>12</sub> particles was barely influenced by the addition of Na<sub>2</sub>O–

Al<sub>2</sub>O<sub>3</sub>–4SiO<sub>2</sub>, the particle surfaces were covered with glass and the grain boundaries and cavities (pores) were filled with the glass with an increase in the amount of Na<sub>2</sub>O–Al<sub>2</sub>O<sub>3</sub>–4SiO<sub>2</sub>.

### 4. Electrical properties

Complex plane impedance plots for Na<sub>3</sub>Zr<sub>2</sub>Si<sub>2</sub>PO<sub>12</sub> are shown in Fig. 2. In a lower-temperature region, the low-frequency results are represented by nearly straight lines and the high-frequency ones by arcs. With an increase in the measuring temperature, the arcs diminished and only quasi-straight lines were observed. Similar characteristics were confirmed for the composite systems. From these observed results the resistance component at each temperature was derived from an extrapolation to zero reactance ( $Z''$ ) of the impedance plot.

Typical Arrhenius plots obtained in the temperature region from room temperature to 330°C are shown in Figs 3 and 4. The conductivity data were parameterized by the Arrhenius equation:

$$\sigma T = \sigma_0 \exp(-E/kT) \quad (1)$$

where  $\sigma$  is the conductivity,  $\sigma_0$  is the pre-exponential factor,  $E$  is the activation energy,  $k$  is the Boltzmann constant and  $T$  is the absolute temperature. For the sample with a higher content of Na<sub>3</sub>Zr<sub>2</sub>Si<sub>2</sub>PO<sub>12</sub>, the activation energy for the ionic conduction changes in the temperature range of 450 to 500 K and the activation energy in the higher-temperature region is lower than that in the lower region. On the other hand, no apparent change to the activation energy could be detected for the sample with a lower content of Na<sub>3</sub>Zr<sub>2</sub>Si<sub>2</sub>PO<sub>12</sub>. Subramanian *et al.* [11] have reported that the good linear relationship between  $\log \sigma$  and  $1/T$  was observed for scandium-substituted rhombohedral NASICON(Na<sub>3</sub>Sc<sub>1.5</sub>Zr<sub>0.5</sub>P<sub>1.5</sub>O<sub>12</sub>) and the activation energy and  $\sigma$  at 500 K were estimated to

TABLE I XRD patterns of ceramics fired at 1000°C

Na <sub>3</sub> Zr <sub>2</sub> Si <sub>2</sub> PO <sub>12</sub>		NASICON-10NA4S		NASICON-20NA4S		NASICON-30NA4S		NASICON-60NA4S		NA4S fired at 1250°C	
$d$ (Å)	$I/I_0$	$d$ (Å)	$I/I_0$	$d$ (Å)	$I/I_0$	$d$ (Å)	$I/I_0$	$d$ (Å)	$I/I_0$	$d$ (Å)	$I/I_0$
6.53	36	6.53	39	6.53	39	6.35	29	6.42	33	5.24	30
4.66	74	4.65	91	4.65	98	4.59	73	5.01	13	4.98	44
4.54	66	4.55	91	4.55	83	4.48	66	4.66	80	4.58	42
3.91	43	3.90	54	3.89	52	3.87	44	4.54	80	4.31	77
3.70	21	3.70	20	3.69	17	3.68	20	4.18	23	4.17	96
3.64	11	3.64	11	3.65	13	3.62	12	3.90	43	3.83	100
3.24	57	3.24	65	3.24	67	3.23	63	3.70	20	3.65	54
3.17	81	3.17	76	3.17	74	3.16	76	3.23	63	3.47	62
2.94	100	2.94	100	2.93	100	2.93	100	3.16	100	3.34	70
2.84	66	2.84	57	2.84	52	2.84	54	3.00	23	3.26	85
2.61	89	2.61	83	2.61	78	2.61	80	2.94	93	3.00	80
2.54	17	2.54	15	2.54	15	2.54	15	2.84	57	2.88	52
2.21	17	2.21	13	2.21	11	2.21	15	2.61	67	2.65	32
2.17	19	2.18	17	2.17	17	2.17	15	2.54	20	2.55	47
		2.05	13	2.05	13	2.06	12			2.49	32
2.03	26	2.03	24	2.03	24	2.03	17	2.34	13	2.38	30
1.97	13	1.97	13	1.97	13	1.98	12	2.30	13	2.34	50
1.95	32	1.95	30	1.95	28	1.95	24	2.21	10	2.30	35
1.85	17	1.85	20	1.85	13	1.85	17	2.17	10	2.24	22
								2.03	17	2.12	26
								1.95	27	2.08	51
								1.84	17	1.98	22

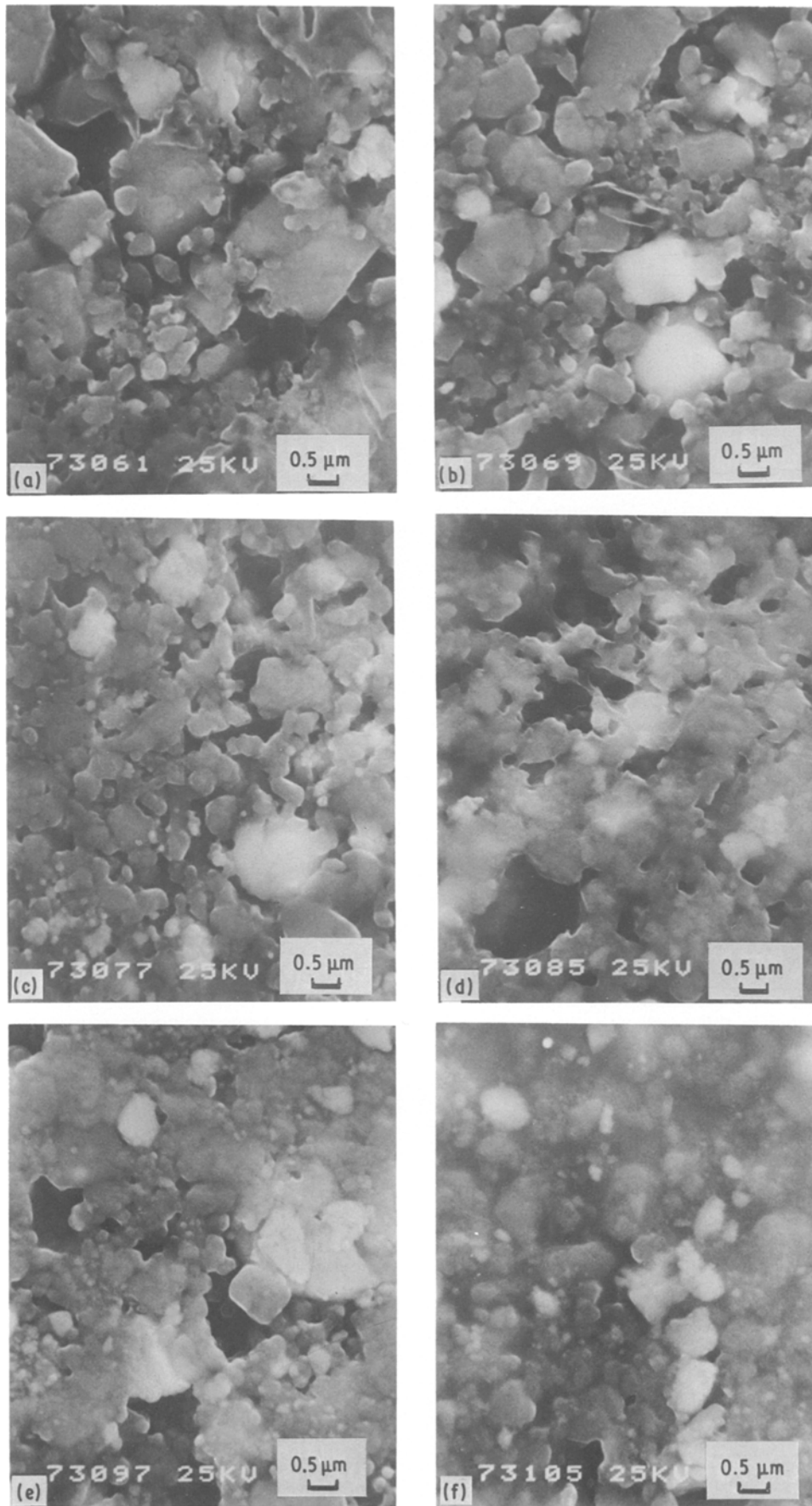


Figure 1 Scanning electron micrographs of fired samples. (a) NASICON, (b) NASICON-10NA4S, (c) NASICON-20NA4S, (d) NASICON-30NA4S, (e) NASICON-40NA4S, (f) NASICON-50NA4S.

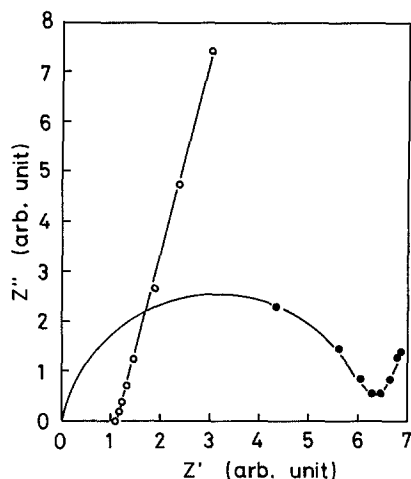


Figure 2 Complex impedance plots for  $\text{Na}_3\text{Zr}_2\text{Si}_2\text{PO}_{12}$ : (●)  $60^\circ\text{C}$ , (○)  $150^\circ\text{C}$ .

be  $0.33\text{ eV}$  and  $\text{ca. } 0.01\text{ S cm}^{-1}$ , respectively. The characteristic values reported are comparable to those for NASICON-30NA4S and NASICON-30NA6S in this work. As shown, addition of sodium aluminosilicates to  $\text{Na}_3\text{Zr}_2\text{Si}_2\text{PO}_{12}$  is a useful method to improve the linearity in the conductivity of crystalline superionic conductors especially in a lower temperature region, while sodium aluminosilicate itself has a very much lower conductivity and a higher activation energy for ionic conduction.

In Figs 5 and 6, the relationship between  $\sigma_0$  and activation energy is shown. These results indicate that  $\log \sigma_0$  decreases with the activation energy and can be divided into two groups, as shown in Figs 5 and 6. For the sample with a higher content of sodium aluminosilicate, above  $\text{ca. } 30\text{ wt}\%$ , the slope in this relationship is considerably lower than that for the sample with a lower content and no distinct changes of activation energy are confirmed, at least in the overall temperature region in this work. On the other hand, for the sample with a lower content of sodium aluminosilicate, the activation energy changes are con-

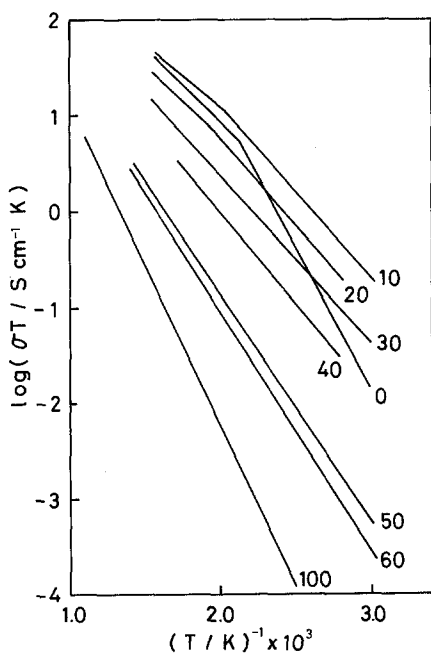


Figure 3 Temperature dependence of  $\sigma T$  for NASICON-XNA4S.  $X(\text{wt}\%)$  is indicated in the figure.

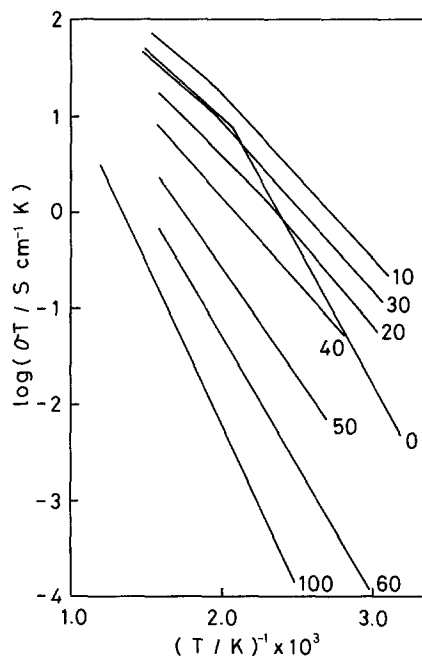


Figure 4 Temperature dependence of  $\sigma T$  for NASICON-XNA6S.  $X(\text{wt}\%)$  is indicated in the figure.

firmed and the relationship between  $\log \sigma_0$  and activation energy determined in both temperature regions expressed by a straight line. Furthermore, the activation energy determined in both higher- and lower-temperature regions was lowered with an increase in sodium aluminosilicate. The linear relationship indicated in Figs 5 and 6 for each case means that the conductivity is expressed as follows:

$$\sigma T = \sigma_0^* \exp(E/kT^*) \exp(-E/kT) \quad (2)$$

where  $\sigma_0^*$  is the pre-exponential factor and  $T^*$  is a characteristic temperature. Equation 2 is well known as the Meyer-Neldel rule [12]. This rule is an empirical relationship which has been reported in very many different materials including many types of semiconductors and ionically conducting materials [13–18]. In general, the conductivity is expressed as:

$$\sigma = Ne\mu \quad (3)$$

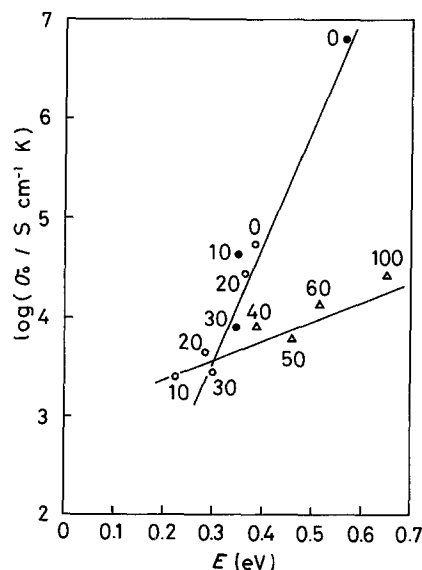


Figure 5 Relationship between  $\log \sigma_0$  and activation energy for NASICON-XNA4S.  $X(\text{wt}\%)$  is shown in the figure. (●), lower temperature region ( $\leq 170^\circ\text{C}$ ), (○) higher region ( $\geq 220^\circ\text{C}$ ), ( $\Delta$ ) whole region.

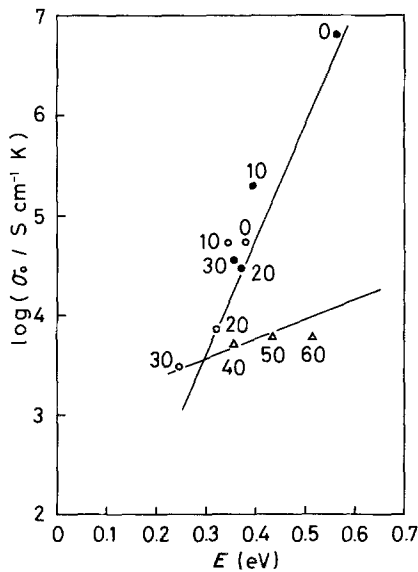


Figure 6 Relationship between  $\log \sigma_0$  and activation energy for NASICON-XNA6S.  $X(\text{wt}\%)$  is shown in the figure. (●), lower temperature region ( $\leq 170^\circ\text{C}$ ), (○) higher region ( $\geq 220^\circ\text{C}$ ), (Δ), whole region.

where  $N$  is the concentration of mobile carrier,  $e$  is the electric charge and  $\mu$  is the mobility of the carrier. The concentration of the carrier may be expressed as:

$$N = N_0 \exp(\Delta S_f/k) \exp(-E_f/kT) \quad (4)$$

and so, the conductivity is expressed as:

$$\sigma = N_0 e^2 d^2 v / gkT \exp[(\Delta S_m + \Delta S_f)/k] \times \exp[-(E_m + E_f)/kT] \quad (5)$$

$$\sigma T = N_0 e^2 d^2 v / gk \exp[(\Delta S_m + \Delta S_f)/k] \times \exp[-(E_m + E_f)/kT] \quad (6)$$

where  $E_f$  and  $\Delta S_f$  are the activation energy and entropy for the carrier creation,  $E_m$  and  $\Delta S_m$  are the activation energy and entropy for the migration of the carrier, respectively. In this model, by assuming that entropy is equal to  $(E_m + E_f)/T^*$ , Equation 2 can be introduced. While there still remains considerable theoretical uncertainty about the origin of the Meyer-Neldel rule, this relationship is useful to examine electrical conduction, since the conductivity and activation energy of a series of superionic conductors composed with crystalline ceramics are related by this relationship which is poorly dependent on composition and may be affected by the phase. For example, the relationship between  $\log \sigma_0$  and the activation energy of NASICON families, which has been summarized by Uvanov and Hairentdinov [19], is shown in Fig. 7. All of these samples are crystalline ceramics. These results are summarized by Equation 2 and are fairly in agreement with this work for the samples with a higher content of  $\text{Na}_3\text{Zr}_2\text{Si}_2\text{PO}_{12}$ . Furthermore, Fig. 7 shows the relationship between  $\log \sigma_0$  and activation energy of a series of sodium aluminosilicates in which  $\text{Na}_2\text{O}/\text{Al}_2\text{O}_3$  ratio is less than unity [6]. In Fig. 7, the straight line determined in this work for the samples with a higher content of sodium aluminosilicate is indicated. It is clear that the characteristics reported previously fit the straight line and the slope of this line is considerably smaller than for crystalline superionic conductors.

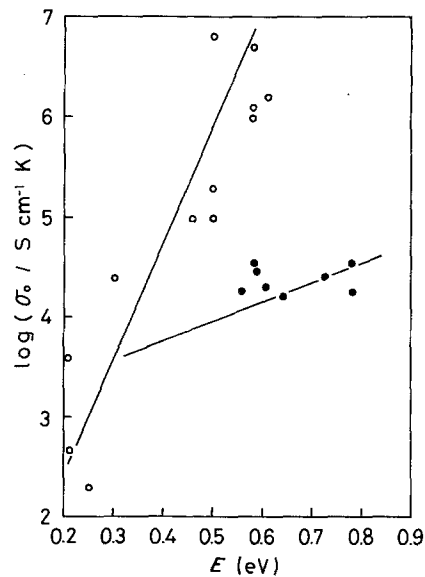


Figure 7 Relationship between  $\log \sigma_0$  and activation energy. (○), crystalline sodium superionic conductor [19], (●) sodium aluminosilicates [6].

## 5. Conclusions

Based on these results it was clarified as follows:

1. Electrical conductivity of most of sodium ion superionic conductor was summarized by the Meyer-Neldel equation and the characteristics determined in high- and low-temperature region for  $\text{Na}_3\text{Zr}_2\text{Si}_2\text{PO}_{12}$  and its composites with a lower content of sodium aluminosilicate were fitted to this equation, confirmed in a series of crystalline superionic conductors.
2. The activation energy changes with temperature for  $\text{Na}_3\text{Zr}_2\text{Si}_2\text{PO}_{12}$  can be depressed by the doping of sodium aluminosilicate and the conductivity in a lower temperature region is enhanced by doping of sodium aluminosilicate of 30 wt % or below.
3. The activation energy for sodium aluminosilicate glass is lowered to ca. 0.35 eV without any distinct reduction of the pre-exponential factor by adding  $\text{Na}_3\text{Zr}_2\text{Si}_2\text{PO}_{12}$  crystal; the crystalline particles are completely covered by sodium aluminosilicate glass without any deformation of  $\text{Na}_3\text{Zr}_2\text{Si}_2\text{PO}_{12}$ .

This paper has focused almost entirely on an empirical approach to make sodium a superionic conductor for electro-chemical applications. However, several new and important correlations concern the effects of phases on ionic conductivity and further experimental and theoretical investigations are now in progress.

## References

1. J. B. GOODENOUGH, H. Y. P. HONG and J. A. KAFALAS, *Mat. Res. Bull.* **11** (1976) 203.
2. U. VON ALPEN, M. F. BELL, R. BRÜTIGAN and H. LAIG-HÖRSTEBROCK, in "Fast Ion Transport in Solids", edited by V. Vashista, J. N. Mundy and G. K. Shenoy (North-Holland Amsterdam, 1979) p. 443.
3. U. VON ALPEN, M. F. BELL and W. WICHEHOUS, *Mat. Res. Bull.* **14** (1979) 1317.
4. R. J. CAVA, E. M. VOGEL and D. W. JOHNSON Jr., *J. Amer. Ceram. Soc.* **65** (1982) C-157.
5. T. TAKAHASHI, K. KUWABARA and M. SHIBATA, *Solid State Ionics* **1** (1980) 163.
6. C. C. HUNTER and M. D. INGRAM, *ibid.* **14** (1984) 31.
7. O. L. ANDERSON and D. A. STUART, *J. Amer.*

- Ceram. Soc.* **37** (1954) 573.
8. M. G. ALEXANDER and B. RILEY, *Solid State Ionics* **18** and **19** (1986) 478.
  9. M. G. ALEXANDER, *ibid.* **22** (1987) 257.
  10. E. BANKS and C. H. KIM, *J. Electrochem. Soc.* **132** (1985) 2617.
  11. M. A. SUBRAMANIAN, P. R. RUDOLF and A. CLEARFIELD, *J. Solid State Chem.* **60** (1985) 172.
  12. W. MEYER and H. NELDEL, *Z. Tech. Phys.* **12** (1937) 588.
  13. R. DEWSBERRY, *J. Phys. D: Appl. Phys.* **8** (1975) 1797.
  14. B. ROSENBERG, B. BHOWMIK, H. C. HARDER and E. POSTOW, *J. Chem. Phys.* **49** (1968) 4108.
  15. K. L. NARASHIMHAN and B. M. ARORA, *Solid State Commun.* **55** (1985) 615.
  16. J. C. DYRE, *J. Phys. C: Solid State Phys.* **19** (1986) 5655.
  17. D. P. ALMOND and A. R. WEST, *Solid State Ionics* **23** (1987) 27.
  18. Y. SADAOKA and Y. SAKAI, *J. Mater. Sci. Lett.* **5** (1986) 656.
  19. N. F. UVANOV and E. F. HAIRENTDINOV, *J. Solid State Chem.* **62** (1986) 1.

*Received 22 January  
and accepted 10 June 1988*